

# Precision Electroweak Tests of the Standard Model

Guido Altarelli  
CERN PH-TH, Geneva 23, Switzerland

Martin W. Grünewald  
Department of Experimental Physics  
University College Dublin, Dublin 4, Ireland

## Abstract

The study of electron-positron collisions at LEP, together with additional measurements from other experiments, in particular those at SLC and at the Tevatron, has allowed for tests of the electroweak Standard Model with unprecedented accuracy. We review the results of the electroweak precision tests and their implications on the determination of the Standard Model parameters, in particular of the Higgs boson mass, and comment on the constraints for possible new physics effects.

*To appear in a special issue of Physics Reports dedicated to CERN  
on the occasion of the laboratory's 50th anniversary*

# 1 Introduction

The experimental study of the electroweak interaction and the Standard Model (SM) has made a quantum leap in the last 15 years. With the advent of electron-positron colliders reaching for the first time centre-of-mass energies of 91 GeV, on-shell production of the Z boson,  $e^+e^- \rightarrow Z$ , allowed precision studies of Z boson properties and the neutral weak current of electroweak interactions. In 1989, two  $e^+e^-$  colliders commenced operations on far away sides of the world: the Stanford Linear Collider (SLC) at SLAC, California, USA, and the circular Large Electron Positron collider (LEP) at CERN, Geneva, Switzerland. While SLC delivered collisions with a longitudinally polarised electron beam, LEP's high luminosity made it a true Z factory.

Five large-scale detectors collected data on  $e^+e^-$  collision processes: SLD at SLC, and ALEPH, DELPHI, L3 and OPAL at LEP. These modern detectors have a typical size of 10m by 10m by 10m, surrounding the interaction region. The detectors' high granularity and near complete hermeticity ensure that all parts of collision events are well measured. Dedicated luminosity monitors using Bhabha scattering at low polar angles measured the luminosity with sub per-mille precision, paving the way for highly precise cross section determinations. Owing to the superior energy and spatial resolution of the five detectors, greatly improved by the subsequent installation of silicon micro-vertex detectors, measurements of observables pertaining to the electroweak interaction have been performed with per-mille precision [1], unprecedented in high energy particle physics outside QED.

This article presents the main results of the programme in electroweak physics at SLC and LEP, covering the measurements at the Z pole but also the second phase of LEP, 1996-2000, where W boson properties were determined based on on-shell W-pair production,  $e^+e^- \rightarrow W^+W^-$ . We put the measurements by SLD and the four LEP experiments together with relevant measurements performed at other colliders; most notably the results from the experiments CDF and DØ, which are taking data at the proton-antiproton collider Tevatron, on the mass of W boson and top quark [2, 3].

## 2 The Z Boson

The process of electron-positron annihilation into fermion-antifermion pairs proceeds via virtual photon and Z boson exchange. As shown in Figure 1, the cross section is dominated by the resonant formation of the Z boson at centre-of-mass energies close to the mass of the Z boson. While SLC mostly studied collisions at the peak energy to maximize event yield, LEP scanned the centre-of-mass energy region from 88 GeV to 94 GeV. A total of 15.5 million hadronic events and 1.7 million lepton-pair events have been recorded by the four LEP experiments, while SLD collected 0.6 million events with longitudinal polarisation of the electron beam in excess of 70%. The three charged lepton species are analysed separately, while the five kinematically accessible quark flavours are treated inclusively in the hadronic final state. Special tagging methods exploiting heavy-quark properties allow the separation of samples highly enriched in Z decays to  $b\bar{b}$  and  $c\bar{c}$  pairs, and thus the determination of partial decay widths and asymmetries for the corresponding heavy-quark flavours.

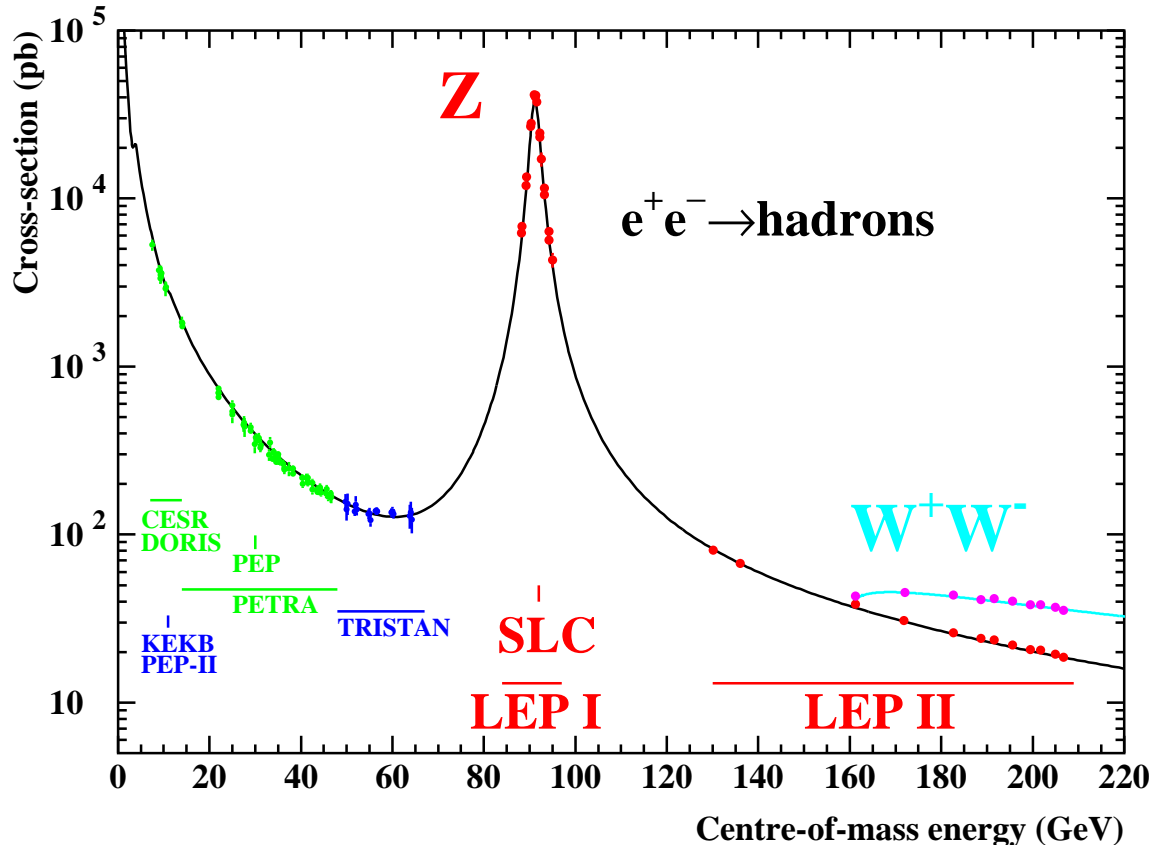


Figure 1: The cross-section for the production of hadrons in  $e^+e^-$  annihilations. The measurements are shown as dots with error bars. The solid line shows the prediction of the SM.

Analysing the resonant Z lineshape in the various Z decay modes leads to the determination of mass, total and partial decay widths of the Z boson as parametrised by a relativistic Breit-Wigner with an  $s$  dependent total width,  $m_Z$ ,  $\Gamma_Z$  and  $\Gamma_{ff}$ . Owing to the precise determination of the LEP beam energy, mass and total width of the Z resonance are now known at the MeV level; the combination of all results yields:

$$m_Z = 91.1875 \pm 0.0021 \text{ GeV} \quad (1)$$

$$\Gamma_Z = 2.4952 \pm 0.0023 \text{ GeV}. \quad (2)$$

Note that the relative accuracy of  $m_Z$  is in the same order as that of the Fermi constant  $G_F$ . The total width  $\Gamma_Z$  corresponds to a lifetime  $\tau_Z = (2.6379 \pm 0.0024)10^{-25}s$ .

An important aspect of the Z lineshape analysis is the determination of the number of light neutrino flavours coupling to the Z boson. The result is:

$$N_\nu = 2.9841 \pm 0.0083, \quad (3)$$

about 1.9 standard deviations less than 3. This result shows that there are just the known

Observable	Measurement	SM fit
$m_Z$ [GeV]	$91.1875 \pm 0.0021$	91.1873
$\Gamma_Z$ [GeV]	$2.4952 \pm 0.0023$	2.4965
$\sigma_h^0$ [nb]	$41.540 \pm 0.037$	41.481
$R_\ell^0$	$20.767 \pm 0.025$	20.739
$A_{\text{FB}}^{0,\ell}$	$0.0171 \pm 0.0010$	0.0164
$\mathcal{A}_\ell$ (SLD)	$0.1513 \pm 0.0021$	0.1480
$\mathcal{A}_\ell (P_\tau)$	$0.1465 \pm 0.0033$	0.1480
$R_b^0$	$0.21644 \pm 0.00065$	0.21566
$R_c^0$	$0.1718 \pm 0.0031$	0.1723
$A_{\text{FB}}^{0,b}$	$0.0995 \pm 0.0017$	0.1037
$A_{\text{FB}}^{0,c}$	$0.0713 \pm 0.0036$	0.0742
$\mathcal{A}_b$	$0.922 \pm 0.020$	0.935
$\mathcal{A}_c$	$0.670 \pm 0.026$	0.668
$\sin^2 \theta_{\text{eff}}^{\text{lept}} (Q_{\text{FB}}^{\text{had}})$	$0.2324 \pm 0.0012$	0.23140
$m_W$ [GeV]	$80.425 \pm 0.034$	80.398
$\Gamma_W$ [GeV]	$2.133 \pm 0.069$	2.094
$m_t$ [GeV] (p $\bar{p}$ [3])	$178.0 \pm 4.3$	178.1
$\Delta\alpha_{\text{had}}^{(5)}(m_Z^2)$ [4]	$0.02761 \pm 0.00036$	0.02768

Table 1: Summary of electroweak precision measurements at high  $Q^2$  [1]. The first block shows the Z-pole measurements. The second block shows additional results from other experiments: the mass and the width of the W boson measured at the Tevatron and at LEP-2, the mass of the top quark measured at the Tevatron, and the contribution to  $\alpha(m_Z^2)$  of the hadronic vacuum polarisation. For the correlations between the measurements, taken into account in our analysis, see [1]. The SM fit results are derived from the SM analysis of these 18 results, also including constants such as the Fermi constant  $G_F$  (fit 3 of Table 2), using the programs TOPAZ0 [5] and ZFITTER [6].

three flavours; hence there exist only the three known sequential generations of fermions (with light neutrinos), a result with important consequences in astrophysics and cosmology.

All electroweak Z pole measurements, combining the results of the 5 experiments, are summarised in Table 1. The cross section scale is given by the pole cross sections for the various final states  $\sigma^0$ ; ratios thereof correspond to ratios of partial decay widths:

$$\sigma_h^0 = \frac{12\pi}{m_Z^2} \frac{\Gamma_{ee}\Gamma_{\text{had}}}{\Gamma_Z^2}, \quad R_\ell^0 = \frac{\sigma_h^0}{\sigma_\ell^0} = \frac{\Gamma_{\text{had}}}{\Gamma_{\ell\ell}}, \quad R_q^0 = \frac{\Gamma_{q\bar{q}}}{\Gamma_{\text{had}}}. \quad (4)$$

Here  $\Gamma_{\ell\ell}$  is the partial decay width for a pair of massless charged leptons. The partial decay

width for a given fermion species contains information about the effective vector and axial-vector coupling constants of the neutral weak current:

$$\Gamma_{ff} = N_C^f \frac{G_F m_Z^3}{6\sqrt{2}\pi} (g_{Af}^2 C_{Af} + g_{Vf}^2 C_{Vf}) + \Delta_{\text{ew/QCD}}, \quad (5)$$

where  $N_C^f$  is the QCD colour factor,  $C_{\{A,V\}f}$  are final-state QCD/QED correction factors also absorbing imaginary contributions to the effective coupling constants,  $g_{Af}$  and  $g_{Vf}$  are the real parts of the effective couplings, and  $\Delta$  contains non-factorisable mixed corrections.

Besides total cross sections, various types of asymmetries have been measured. The results of all asymmetry measurements are quoted in terms of the asymmetry parameter  $\mathcal{A}_f$ , defined in terms of the real parts of the effective coupling constants,  $g_{Vf}$  and  $g_{Af}$ , as:

$$\mathcal{A}_f = 2 \frac{g_{Vf} g_{Af}}{g_{Vf}^2 + g_{Af}^2} = 2 \frac{g_{Vf}/g_{Af}}{1 + (g_{Vf}/g_{Af})^2}, \quad A_{\text{FB}}^{0,f} = \frac{3}{4} \mathcal{A}_e \mathcal{A}_f. \quad (6)$$

The measurements are: the forward-backward asymmetry ( $A_{\text{FB}}^{0,f} = (3/4)\mathcal{A}_e \mathcal{A}_f$ ), the tau polarisation ( $\mathcal{A}_\tau$ ) and its forward backward asymmetry ( $\mathcal{A}_e$ ) measured at LEP, as well as the left-right and left-right forward-backward asymmetry measured at SLC ( $\mathcal{A}_e$  and  $\mathcal{A}_f$ , respectively). Hence the set of partial width and asymmetry results allows the extraction of the effective coupling constants. An overview comparing all fermion species in the  $(g_{Af}, g_{Vf})$  plane is given in Figure 2 left, while an expanded view of the leptonic couplings is given in Figure 2 right. Compared to the situation in 1987, the accuracy of the effective coupling constants has improved by more than a factor of 100. Lepton universality of the neutral weak current is now established at the per-mille level.

Using the effective electroweak mixing angle,  $\sin^2 \theta_{\text{eff}}^f$ , and the  $\rho$  parameter, the effective coupling constants are given by:

$$g_{Af} = \sqrt{\rho} T_3^f, \quad \frac{g_{Vf}}{g_{Af}} = 1 - 4|q_f| \sin^2 \theta_{\text{eff}}^f, \quad (7)$$

where  $T_3^f$  is the third component of the weak iso-spin and  $q_f$  the electric charge of the fermion. The effective electroweak mixing angle is thus given independently of the  $\rho$  parameter by the ratio  $g_{Vf}/g_{Af}$  and hence in a one-to-one relation by each asymmetry result.

The various asymmetries determine the effective electroweak mixing angle for leptons with highest sensitivity. The results on  $\sin^2 \theta_{\text{eff}}^{\text{lept}}$  are compared in Figure 3. The weighted average of these six results, including small correlations, is:

$$\sin^2 \theta_{\text{eff}}^{\text{lept}} = 0.23150 \pm 0.00016. \quad (8)$$

Note, however, that this average has a  $\chi^2$  of 10.5 for 5 degrees of freedom, corresponding to a probability of 6.2%. The  $\chi^2$  is pushed up by the two most precise measurements of

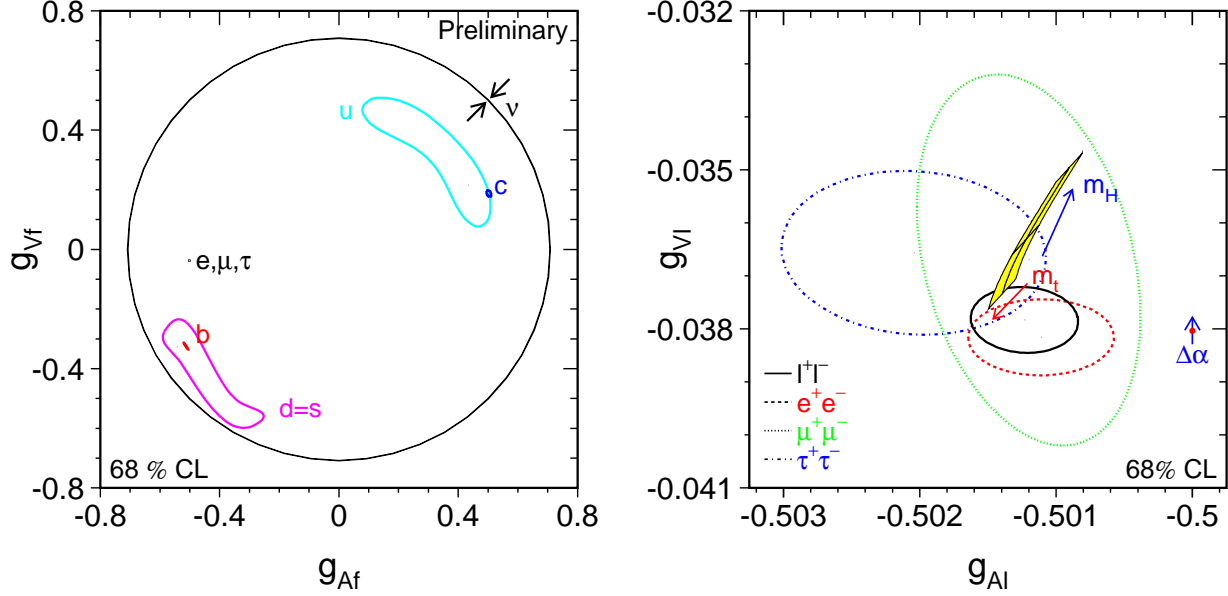


Figure 2: Left: Effective vector and axial-vector coupling constants for fermions. For light quarks, identical couplings for d and s quarks are assumed in the analysis. The allowed area for neutrinos, assuming three generations of neutrinos with identical vector and axial-vector couplings, is a thin ring bounded by two virtually identical circles centred at the origin. On the scale of the left plot, the SM expectation of up and down type quarks lie on top of the b and c allowed regions. Right: Effective vector and axial-vector coupling constants for leptons. The shaded region in the lepton plot shows the predictions within the SM for  $m_t = 178.0 \pm 4.3$  GeV and  $m_H = 300_{-186}^{+700}$  GeV; varying the hadronic vacuum polarisation by  $\Delta\alpha_{\text{had}}^{(5)}(m_Z^2) = 0.02761 \pm 0.00036$  yields an additional uncertainty on the SM prediction shown by the arrow labelled  $\Delta\alpha$ .

$\sin^2 \theta_{\text{eff}}^{\text{lept}}$ , namely those derived from the measurements of  $\mathcal{A}_\ell$  by SLD, dominated by the left-right asymmetry  $A_{\text{LR}}^0$ , and of the forward-backward asymmetry measured in  $b\bar{b}$  production at LEP,  $A_{\text{FB}}^{0,b}$ , which differ by about 2.9 standard deviations. No experimental effect in either measurement has been identified to explain this, thus the difference is presumably either a statistical fluctuation or a hint for new physics, further discussed below.

### 3 The W Boson

With the installation of superconducting RF cavities, the centre-of-mass energy for  $e^+e^-$  collisions provided by LEP was more than doubled. From 1996 to the end of LEP running in the year 2000, the centre-of-mass energy increased from 160 GeV, the kinematic threshold of W-pair production, up to 209 GeV. More than 40,000 W-pair events in all W decay modes,  $W^+W^- \rightarrow q\bar{q}q\bar{q}$ ,  $W^+W^- \rightarrow q\bar{q}\ell\nu_\ell$  and  $W^+W^- \rightarrow \ell\nu_\ell\ell\nu_\ell$ , have been recorded by the four LEP experiments. Among the many measurements of W boson properties, the W-pair production cross section and the mass and total width of the W boson are of central importance to the

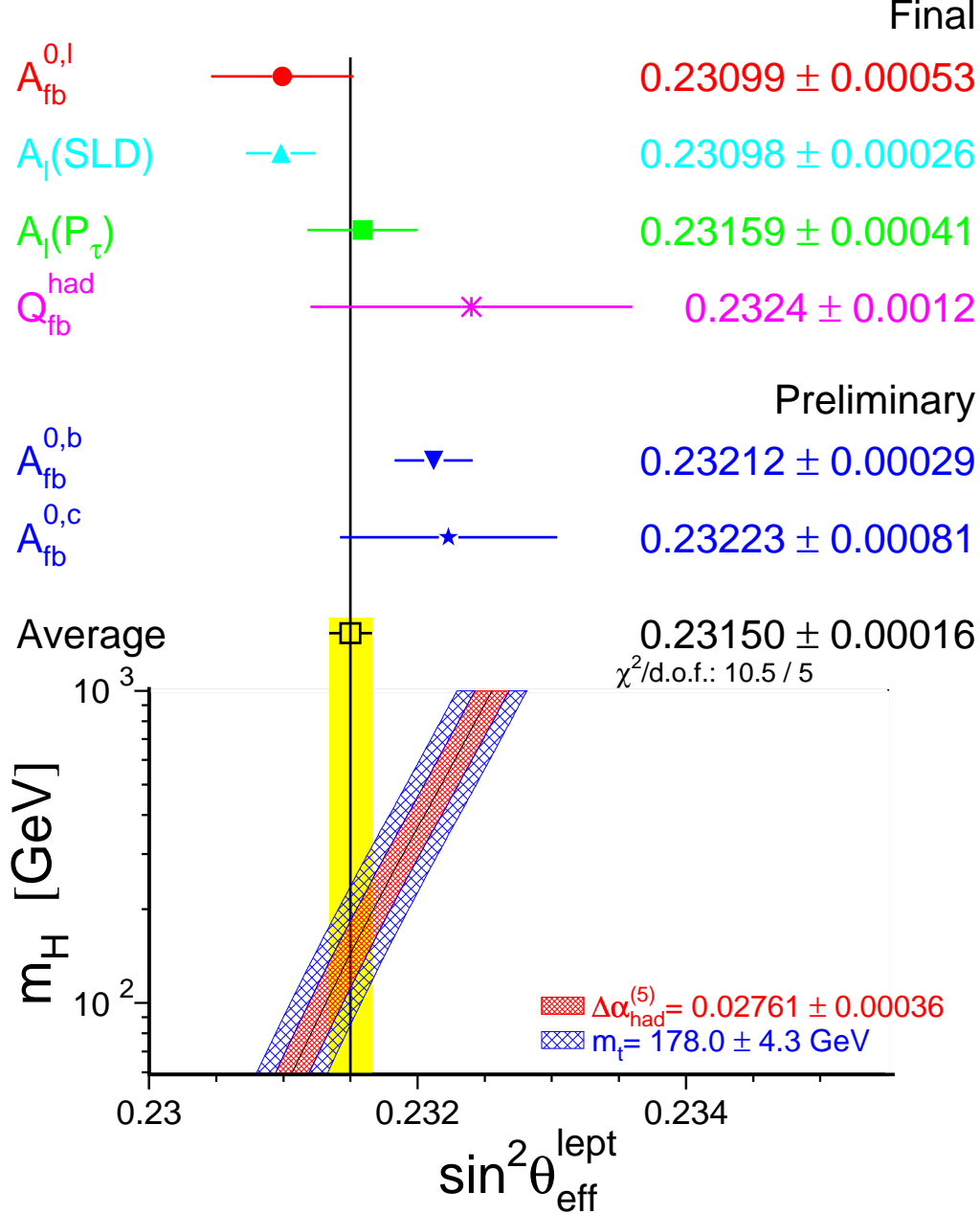


Figure 3: Effective electroweak mixing angle  $\sin^2 \theta_{\text{eff}}^{\text{lept}}$  derived from measurement results depending on lepton couplings only (top) and also quark couplings (bottom). Also shown is the prediction of  $\sin^2 \theta_{\text{eff}}^{\text{lept}}$  in the SM as a function of  $m_H$ , including its parametric uncertainty dominated by the uncertainties in  $\Delta\alpha_{\text{had}}^{(5)}(m_Z^2)$  and  $m_t$ , shown as the bands.

electroweak SM.

The cross section for W-pair production is shown in Figure 4 [1]. Trilinear gauge couplings between the electroweak gauge bosons  $\gamma$ , W and Z, as predicted by the electroweak SM, are required to explain the cross sections measured as a function of  $\sqrt{s}$ . The mass and width of the W boson is measured by reconstructing the invariant mass of its decay products. Monte Carlo events generated with a known W-boson mass distribution are reweighted in order to

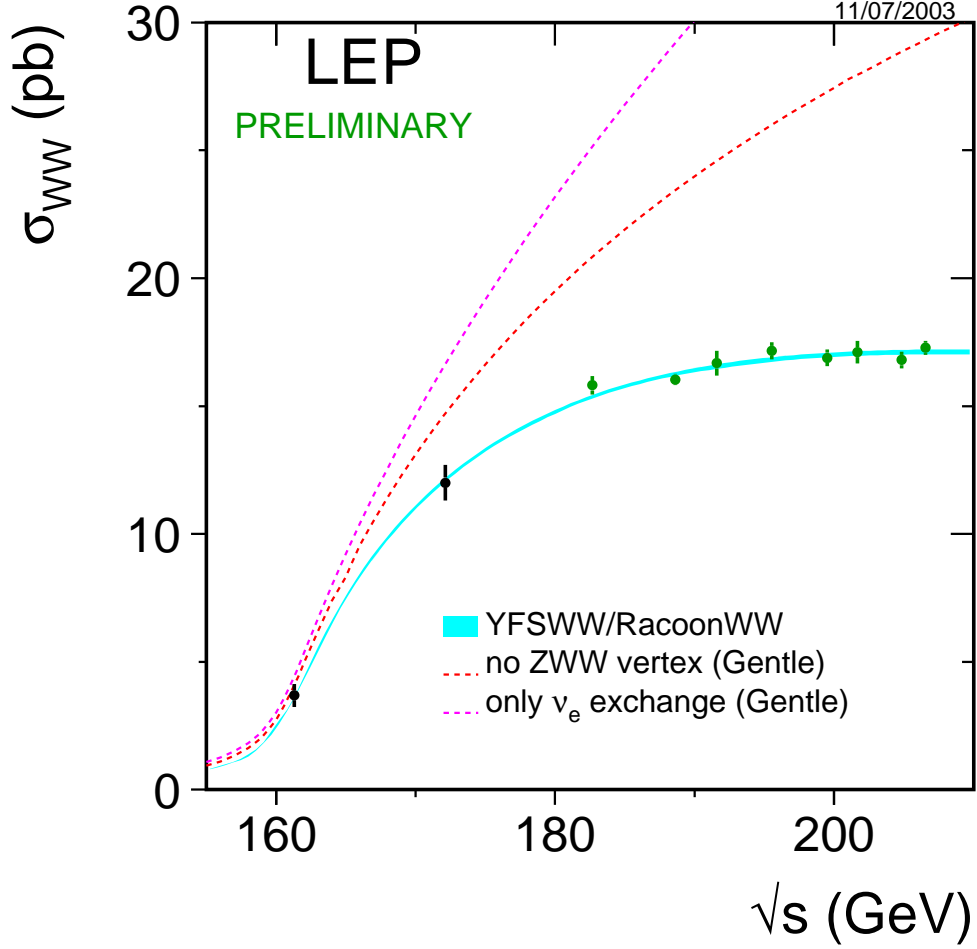


Figure 4: The measured W-pair production cross section compared to the SM and alternative theories not including trilinear gauge couplings.

obtain the best fit to the distribution observed in data, yielding a measurement of  $m_W$  and  $\Gamma_W$ . The events of the type  $W^+W^- \rightarrow q\bar{q}\ell\nu_\ell$  dominate the mass determination. The channel  $W^+W^- \rightarrow q\bar{q}q\bar{q}$  is less precise due to potentially large final-state interconnection effects arising from cross talk between the two hadronic systems of the decaying W bosons. Effects such as colour reconnection, or Bose-Einstein correlation effects between final-state hadrons, may spoil the identification of the invariant mass of the decay products with the invariant mass of the decaying W bosons.

Combining all LEP-2 results, most still preliminary, the best values are [1]:

$$m_W = 80.412 \pm 0.042 \text{ GeV} \quad (9)$$

$$\Gamma_W = 2.150 \pm 0.091 \text{ GeV}, \quad (10)$$

in very good agreement with the results from the CDF and DØ experiments at the Tevatron collider [2]. The combined LEP-2 and Tevatron results are reported in Table 1.



## 4 Interpretation within the Standard Model

For the analysis of electroweak data in the SM one starts from the input parameters: as in any renormalisable theory masses and couplings have to be specified from outside. One can trade one parameter for another and this freedom is used to select the best measured ones as input parameters. As a result, some of them,  $\alpha$ ,  $G_F$  and  $m_Z$ , are very precisely known, some other ones,  $m_{flight}$ ,  $m_t$  and  $\alpha_s(m_Z)$  are far less well determined while  $m_H$  is largely unknown. Note that the new combined CDF and DØ value for  $m_t$  [3], as listed in Table 1, is higher than the previous average by nearly one standard deviation.

Among the light fermions, the quark masses are badly known, but fortunately, for the calculation of radiative corrections, they can be replaced by  $\alpha(m_Z)$ , the value of the QED running coupling at the Z mass scale. The value of the hadronic contribution to the running,  $\Delta\alpha_{had}^{(5)}(m_Z^2)$ , reported in Table 1, is obtained through dispersion relations from the data on  $e^+e^- \rightarrow \text{hadrons}$  at low centre-of-mass energies [4]. From the input parameters one computes the radiative corrections to a sufficient precision to match the experimental accuracy. Then one compares the theoretical predictions and the data for the numerous observables which have been measured, checks the consistency of the theory and derives constraints on  $m_t$ ,  $\alpha_s(m_Z^2)$  and  $m_H$ .

The computed radiative corrections include the complete set of one-loop diagrams, plus some selected large subsets of two-loop diagrams and some sequences of resummed large terms of all orders (large logarithms and Dyson resummations). In particular large logarithms, e.g., terms of the form  $(\alpha/\pi \ln(m_Z/m_{f_\ell}))^n$  where  $f_\ell$  is a light fermion, are resummed by well-known and consolidated techniques based on the renormalisation group. For example, large logarithms dominate the running of  $\alpha$  from  $m_e$ , the electron mass, up to  $m_Z$ , which is a 6% effect, much larger than the few per-mille contributions of purely weak loops. Also, large logs from initial state radiation dramatically distort the line shape of the Z resonance observed at LEP-1 and SLC and must be accurately taken into account in the measurement of the Z mass and total width.

Among the one loop EW radiative corrections a remarkable class of contributions are those terms that increase quadratically with the top mass. The large sensitivity of radiative corrections to  $m_t$  arises from the existence of these terms. The quadratic dependence on  $m_t$  (and possibly on other widely broken isospin multiplets from new physics) arises because, in spontaneously broken gauge theories, heavy loops do not decouple. On the contrary, in QED or QCD, the running of  $\alpha$  and  $\alpha_s$  at a scale  $Q$  is not affected by heavy quarks with mass  $M \gg Q$ . According to an intuitive decoupling theorem [7], diagrams with heavy virtual particles of mass  $M$  can be ignored for  $Q \ll M$  provided that the couplings do not grow with  $M$  and that the theory with no heavy particles is still renormalizable. In the spontaneously broken EW gauge theories both requirements are violated. First, one important difference with respect to unbroken gauge theories is in the longitudinal modes of weak gauge bosons. These modes are generated by the Higgs mechanism, and their couplings grow with masses (as is also the case for the physical Higgs couplings). Second, the theory without the top quark is no more renormalisable because the gauge symmetry is broken if the b quark is left with no partner (while its couplings show that the weak isospin is 1/2). Because of non decoupling precision tests of the electroweak theory may be sensitive to new physics even if the new particles are

Fit	1	2	3
Measurements	$m_W, \Gamma_W$	$m_t$	$m_t, m_W, \Gamma_W$
$m_t$ (GeV)	$178.5^{+11.0}_{-8.5}$	$177.2 \pm 4.1$	$178.1 \pm 3.9$
$m_H$ (GeV)	$117^{+162}_{-62}$	$129^{+76}_{-50}$	$113^{+62}_{-42}$
$\log [m_H(\text{GeV})]$	$2.07^{+0.38}_{-0.33}$	$2.11 \pm 0.21$	$2.05 \pm 0.20$
$\alpha_s(m_Z)$	$0.1187 \pm 0.0027$	$0.1190 \pm 0.0027$	$0.1186 \pm 0.0027$
$\chi^2/dof$	16.3/12	15.0/11	16.3/13
$m_W$ (MeV)		$80386 \pm 23$	

Table 2: Standard Model fits of electroweak data. All fits use the Z pole results and  $\Delta\alpha_{\text{had}}^{(5)}(m_Z^2)$  as listed in Table 1, also including constants such as the Fermi constant  $G_F$ . In addition, the measurements listed in each column are included as well. For fit 2, the expected W mass is also shown. For details on the fit procedure, using the programs TOPAZ0 [5] and ZFITTER [6], see [1].

too heavy for their direct production.

While radiative corrections are quite sensitive to the top mass, they are unfortunately much less dependent on the Higgs mass. If they were sufficiently sensitive, by now we would precisely know the mass of the Higgs. However, the dependence of one loop diagrams on  $m_H$  is only logarithmic:  $\sim G_F m_W^2 \log(m_H^2/m_W^2)$ . Quadratic terms  $\sim G_F^2 m_H^2$  only appear at two loops and are too small to be important. The difference with the top case is that  $m_t^2 - m_b^2$  is a direct breaking of the gauge symmetry that already affects the relevant one loop diagrams, while the Higgs couplings to gauge bosons are "custodial-SU(2)" symmetric in lowest order.

We now discuss fitting the data in the SM. One can think of different types of fit, depending on which experimental results are included or which answers one wants to obtain. For example, in Table 2 we present in column 1 a fit of all Z pole data plus  $m_W$  and  $\Gamma_W$  (this is interesting as it shows the value of  $m_t$  obtained indirectly from radiative corrections, to be compared with the value of  $m_t$  measured in production experiments), in column 2 a fit of all Z pole data plus  $m_t$  (here it is  $m_W$  which is indirectly determined), and, finally, in column 3 a fit of all the data listed in Table 1 (which is the most relevant fit for constraining  $m_H$ ). From the fit in column 1 of Table 2 we see that the extracted value of  $m_t$  is in perfect agreement with the direct measurement (see Table 1). Similarly we see that the experimental measurement of  $m_W$  in Table 1 is larger by about one standard deviation with respect to the value from the fit in column 2. We have seen that quantum corrections depend only logarithmically on  $m_H$ . In spite of this small sensitivity, the measurements are precise enough that one still obtains a quantitative indication of the mass range. From the fit in column 3 we obtain:  $\log_{10} m_H(\text{GeV}) = 2.05 \pm 0.20$  (or  $m_H = 113^{+62}_{-42}$  GeV). This result on the Higgs mass is particularly remarkable. The value of  $\log_{10} m_H(\text{GeV})$  is right on top of the small window between  $\sim 2$  and  $\sim 3$  which is allowed, on the one side, by the direct search limit ( $m_H \gtrsim 114$  GeV from LEP-2 [8]), and, on the other side, by the theoretical upper limit on the Higgs mass in the minimal SM,  $m_H \lesssim 600 - 800$  GeV [9].

Observable	Measurement	SM fit
$\sin^2 \theta_W$ ( $\nu N$ [10])	$0.2277 \pm 0.0016$	0.2226
$Q_W(\text{Cs})$ (APV [11])	$-72.84 \pm 0.49$	-72.91
$\sin^2 \theta_{\text{eff}}^{\text{lept}}$ ( $e^-e^-$ [12])	$0.2296 \pm 0.0023$	0.2314

Table 3: Summary of other electroweak precision measurements, namely the measurements of the on-shell electroweak mixing angle in neutrino-nucleon scattering, the weak charge of cesium measured in an atomic parity violation experiment, and the effective weak mixing angle measured in Moller scattering, all performed in processes at low  $Q^2$ . The SM predictions are derived from fit 3 of Table 2. Good agreement of the prediction with the measurement is found except for  $\nu N$ .

Thus the whole picture of a perturbative theory with a fundamental Higgs is well supported by the data on radiative corrections. It is important that there is a clear indication for a particularly light Higgs: at 95% c.l.  $m_H \lesssim 237$  GeV. This is quite encouraging for the ongoing search for the Higgs particle. More general, if the Higgs couplings are removed from the Lagrangian the resulting theory is non renormalisable. A cutoff  $\Lambda$  must be introduced. In the quantum corrections  $\log m_H$  is then replaced by  $\log \Lambda$  plus a constant. The precise determination of the associated finite terms would be lost (that is, the value of the mass in the denominator in the argument of the logarithm). A heavy Higgs would need some unfortunate conspiracy: the finite terms, different in the new theory from those of the SM, should accidentally compensate for the heavy Higgs in a few key parameters of the radiative corrections (mainly  $\epsilon_1$  and  $\epsilon_3$ , see, for example, [13]). Alternatively, additional new physics, for example in the form of effective contact terms added to the minimal SM lagrangian, should accidentally do the compensation, which again needs some sort of conspiracy.

In Table 3 we collect the results on low energy precision tests of the SM obtained from neutrino and antineutrino deep inelastic scattering (NuTeV [10]), parity violation in Cs atoms (APV [11]) and the recent measurement of the parity-violating asymmetry in Moller scattering [12]. The experimental results are compared with the predictions from the fit in column 3 of Table 2. We see the agreement is good except for the NuTeV result that shows a deviation by three standard deviations. The NuTeV measurement is quoted as a measurement of  $\sin^2 \theta_W = 1 - m_W^2/m_Z^2$  from the ratio of neutral to charged current deep inelastic cross-sections from  $\nu_\mu$  and  $\bar{\nu}_\mu$  using the Fermilab beams. There is growing evidence that the NuTeV anomaly could simply arise from an underestimation of the theoretical uncertainty in the QCD analysis needed to extract  $\sin^2 \theta_W$ . In fact, the lowest order QCD parton formalism on which the analysis has been based is too crude to match the experimental accuracy. In particular a small asymmetry in the momentum carried by the strange and antistrange quarks,  $s - \bar{s}$ , could have a large effect [14]. A tiny violation of isospin symmetry in parton distributions, too small to be seen elsewhere, can similarly be of some importance. In conclusion we believe the discrepancy has more to teach about the QCD parton densities than about the electroweak theory.

When confronted with these results, on the whole the SM performs rather well, so that it is fair to say that no clear indication for new physics emerges from the data. However, as already mentioned, one problem is that the two most precise measurements of  $\sin^2 \theta_{\text{eff}}^{\text{lept}}$

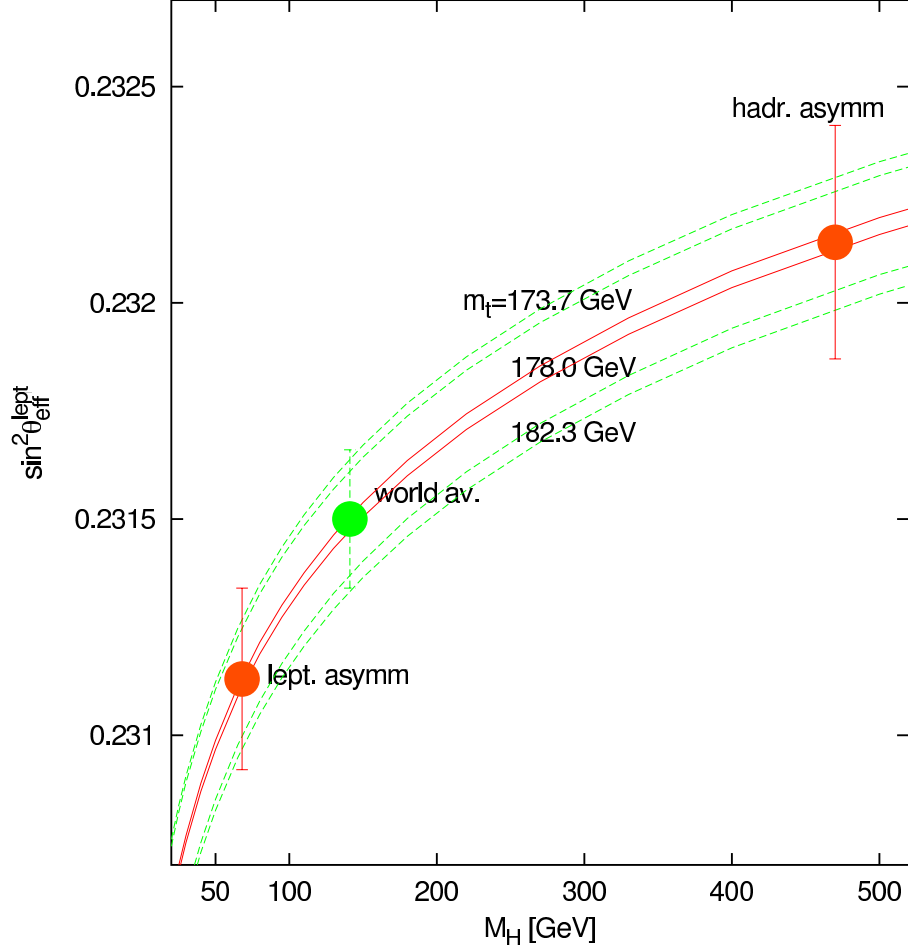


Figure 5: The data for  $\sin^2 \theta_{\text{eff}}^{\text{lept}}$  are plotted vs  $m_H$ . For presentation purposes the measured points are shown each at the  $m_H$  value that would ideally correspond to it given the central value of  $m_t$  (updated from [15]).

from  $A_{\text{LR}}$  and  $A_{\text{FB}}^{0,b}$  differ nearly three standard deviations. In general, there appears to be a discrepancy between  $\sin^2 \theta_{\text{eff}}^{\text{lept}}$  measured from leptonic asymmetries ( $(\sin^2 \theta_{\text{eff}})_l$ ) and from hadronic asymmetries ( $(\sin^2 \theta_{\text{eff}})_h$ ), see also Figure 3. In fact, the result from  $A_{\text{LR}}$  is in good agreement with the leptonic asymmetries measured at LEP, while all hadronic asymmetries, though their errors are large, are better compatible with the result of  $A_{\text{FB}}^{0,b}$ .

The situation is shown in Figure 5 [15]. The values of  $(\sin^2 \theta_{\text{eff}})_l$ ,  $(\sin^2 \theta_{\text{eff}})_h$  and their formal combination are shown each at the  $m_H$  value that would correspond to it given the central value of  $m_t$ . Of course, the value for  $m_H$  indicated by each  $\sin^2 \theta_{\text{eff}}^{\text{lept}}$  has an horizontal ambiguity determined by the measurement error and the width of the  $\pm 1\sigma$  band for  $m_t$ . Even taking this spread into account it is clear that the implications on  $m_H$  are sizably different. One might imagine that some new physics effect could be hidden in the  $Zb\bar{b}$  vertex. Like for the top quark mass there could be other non decoupling effects from new heavy states or a mixing of the  $b$  quark with some other heavy quark. However, it is well known that this discrepancy is not easily explained in terms of some new physics effect in the  $Zb\bar{b}$  vertex. In fact,  $A_{\text{FB}}^{0,b}$  is the product of lepton- and  $b$ -asymmetry factors:  $A_{\text{FB}}^{0,b} = (3/4)\mathcal{A}_e\mathcal{A}_b$ . The sensitivity of  $A_{\text{FB}}^{0,b}$

to  $\mathcal{A}_b$  is limited, because the  $\mathcal{A}_e$  factor is small, so that a rather large change of the b-quark couplings with respect to the SM is needed in order to reproduce the measured discrepancy (precisely a  $\sim 30\%$  change in the right-handed coupling, an effect too large to be a loop effect but which could be produced at the tree level, e.g., by mixing of the b quark with a new heavy vectorlike quark [16]). But then this effect should normally also appear in the direct measurement of  $\mathcal{A}_b$  performed at SLD using the left-right polarized b asymmetry, even within the moderate precision of this result, and it should also be manifest in the accurate measurement of  $R_b \propto g_{Rb}^2 + g_{Lb}^2$ . The measurements of neither  $\mathcal{A}_b$  nor  $R_b$  confirm the need of a new effect. Even introducing an ad hoc mixing the overall fit is not terribly good, but we cannot exclude this possibility completely. Alternatively, the observed discrepancy could be due to a large statistical fluctuation or an unknown experimental problem. The ambiguity in the measured value of  $\sin^2 \theta_{\text{eff}}^{\text{lept}}$  could thus be larger than the nominal error, reported in Equation 8, obtained from averaging all the existing determinations.

We have already observed that the experimental value of  $m_W$  (with good agreement between LEP and the Tevatron) is a bit high compared to the SM prediction (see Figure 6). The value of  $m_H$  indicated by  $m_W$  is on the low side, just in the same interval as for  $\sin^2 \theta_{\text{eff}}^{\text{lept}}$  measured from leptonic asymmetries. It is interesting that the new value of  $m_t$  considerably relaxes the previous tension between the experimental values of  $m_W$  and  $\sin^2 \theta_{\text{eff}}^{\text{lept}}$  measured from leptonic asymmetries on one side and the lower limit on  $m_H$  from direct searches on the other side [17,18]. This is also apparent from Figure 6.

The main lesson of precision tests of the standard electroweak theory can be summarised as follows. The couplings of quark and leptons to the weak gauge bosons  $W^\pm$  and  $Z$  are indeed precisely those prescribed by the gauge symmetry. The accuracy of a few per-mille for these tests implies that, not only the tree level, but also the structure of quantum corrections has been verified. To a lesser accuracy the triple gauge vertices  $\gamma W^+ W^-$  and  $Z W^+ W^-$  have also been found in agreement with the specific prediction of the  $SU(2) \otimes U(1)$  gauge theory. This means that it has been verified that the gauge symmetry is unbroken in the vertices of the theory: the currents are indeed conserved. Yet there is obvious evidence that the symmetry is otherwise badly broken in the masses. Thus the currents are conserved but the spectrum of particle states is not at all symmetric. This is a clear signal of spontaneous symmetry breaking. The practical implementation of spontaneous symmetry breaking in a gauge theory is via the Higgs mechanism. The Higgs sector of the SM is still very much untested. What has been tested is the relation  $m_W^2 = m_Z^2 \cos^2 \theta_W$ , modified by computable radiative corrections. This relation means that the effective Higgs (be it fundamental or composite) is indeed a weak isospin doublet. The Higgs particle has not been found but in the SM its mass can well be larger than the present direct lower limit  $m_H \gtrsim 114$  GeV obtained from direct searches at LEP-2. The radiative corrections computed in the SM when compared to the data on precision electroweak tests lead to a clear indication for a light Higgs, not too far from the present lower bound. No signal of new physics has been found. However, to make a light Higgs natural in presence of quantum fluctuations new physics should not be too far. This is encouraging for the LHC that should experimentally clarify the problem of the electroweak symmetry breaking sector and search for physics beyond the SM.

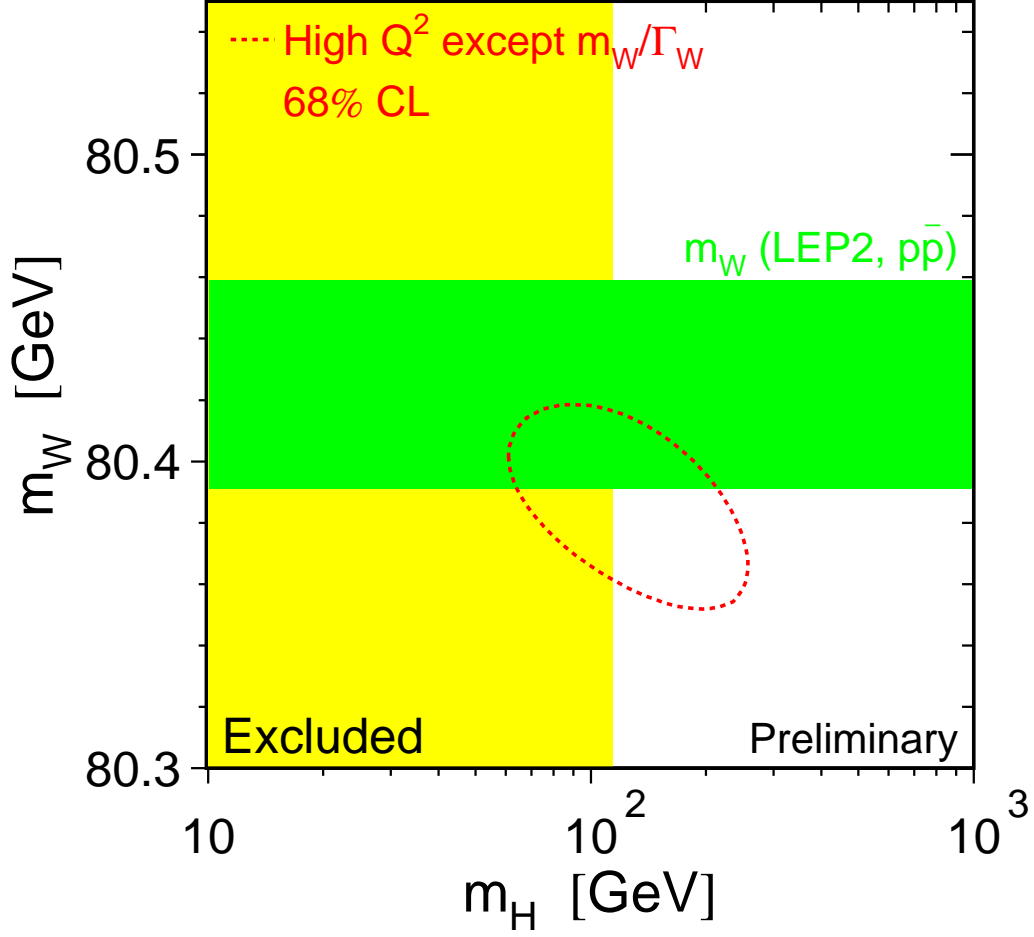


Figure 6: Contour curve of 68% probability in the  $(m_W, m_H)$  plane derived from fit 2 of Table 2. The direct experimental measurement, not included in the fit, is shown as the horizontal band of width  $\pm 1$  standard deviation. The vertical band shows the 95% confidence level exclusion limit on  $m_H$  of 114 GeV [8].

# References

- [1] The ALEPH, DELPHI, L3, OPAL, SLD Collaborations and the LEP Electroweak Working Group, *A Combination of Preliminary Electroweak Measurements and Constraints on the Standard Model*, hep-ex/0312023, and references therein.
- [2] The CDF Collaboration, the DØ Collaboration, and the Tevatron Electroweak Working Group, *Combination of CDF and DØ results on W boson mass and width*, hep-ex/0311039.
- [3] The CDF Collaboration, the DØ Collaboration, and the Tevatron Electroweak Working Group, *Combination of CDF and DØ Results on the Top-Quark Mass*, hep-ex/0404010.
- [4] H. Burkhardt, B. Pietrzyk, *Update of the Hadronic Contribution to the QED Vacuum Polarization*, Phys. Lett. B 513 (2001) 46.
- [5] G. Passarino *et al.*, *TOPAZ0*, CPC 76 (1993) 328, hep-ph/9506329, CPC 93 (1996) 120, hep-ph/9804211, CPC 117 (1999) 278, and references therein.
- [6] D.Y. Bardin *et al.*, *ZFITTER*, hep-ph/9412201, hep-ph/9908433, CPC 133(2001) 229, and references therein.
- [7] Th. Appelquist, J. Carazzone, *Infrared Singularities and Massive Fields*, Phys. Rev. D 11 (1975) 2856.
- [8] The ALEPH, DELPHI, L3 and OPAL Collaborations, and the LEP Working Group for Higgs Boson Searches, *Search for the Standard Model Higgs Boson at LEP*, hep-ex/0306033, Phys. Lett. B 565 (2003) 61-75.
- [9] Th. Hambye, K. Riesselmann, *Matching Conditions and Higgs Mass Upper Bounds Revisited*, hep-ph/9610272, Phys. Rev. D 55 (1997) 7255-7262.
- [10] The NuTeV Collaboration, G.P. Zeller *et al.*, Phys. Rev. Lett. **88** (2002) 091802.
- [11] M. Yu. Kuchiev and V. V. Flambaum, *Radiative Corrections to Parity Non-Conservation in Atoms*, hep-ph/0305053.
- [12] The SLAC E158 Collaboration, P.L. Anthony *et al.*, *Observation of Parity Non-Conservation in Moller scattering*, hep-ex/0312035, *A New Measurement of the Weak Mixing Angle*, hep-ex/0403010. We have added 0.0003 to the value of  $\sin^2\theta(m_Z)$  quoted by E158 in order to convert from the  $\overline{\text{MS}}$  scheme to the effective electroweak mixing angle [19].
- [13] G. Altarelli, R. Barbieri, F. Caravaglios, *Electroweak Precision Tests: A Concise Review*, hep-ph/9712368, Int. Jour. Mod. Phys. A 13 (1998) 1031-1058.
- [14] S. Davidson, S. Forte, P. Gambino, N. Rius, A. Strumia, *Old and New Physics Interpretations of the NuTeV Anomaly*, hep-ph/0112302, JHEP 0202:037, 2002.
- [15] P. Gambino, *The Top Priority: Precision Electroweak Physics from Low-Energy to High-Energy*, hep-ph/0311257.

- [16] D. Choudhury, T.M.P. Tait, C.E.M. Wagner, *Beautiful Mirrors and Precision Electroweak Data*, hep-ph/0109097, Phys. Rev. D 65 (2002) 053002.
- [17] M. S. Chanowitz, *Electroweak Data and the Higgs Boson Mass: A Case for New Physics*, hep-ph/0207123, Phys. Rev. D 66 (2002) 073002.
- [18] G. Altarelli, F. Caravaglios, G.F. Giudice, P. Gambino, G. Ridolfi, *Indication for Light Sneutrinos and Gauginos from Precision Electroweak Data*, hep-ph 0106029, JHEP 0106:018, 2001.
- [19] The Particle Data Group, *Review of Particle Physics*, Phys. Rev. D 66 (2002) 1.